High-rate GNSS Amplitude Estimation Applied to Airborne Observation of In-land Water Body Surfaces

Hamza ISSA[1,2], Georges STIENNE[1], Serge REBOUL[1], Mohamad RAAD[3], Ghaleb FAOUR[2]

[1]Laboratoire d'Informatique, Signal et Image de la Côte d'Opale (LISIC),
Université du Littoral Côte d'Opale (ULCO), Calais, France.

[2]Remote Sensing Research Center,
National Council of Scientific Research (CNRS-L), Mansouriyeh, Lebanon.

[3]School of Engineering,
Lebanese International University (LIU), Beirut, Lebanon.

hamza.issa@univ-littoral.fr, georges.stienne@univ-littoral.fr,
serge.reboul@univ-littoral.fr, mohamad.raad@liu.edu.lb, gfaour@cnrs.edu.lb

Résumé – Cet article présente un modèle pour l'estimation de l'amplitude du signal GNSS qui utilise la corrélation du signal comme observation. Nous estimons les amplitudes à la fréquence de répétition du code des signaux GPS C/A (fréquence de 1 ms). Cependant, le modèle qui relie les observations de la composante en phase à l'amplitude du signal à la fréquence de 1 ms est non linéaire. Pour estimer les amplitudes des signaux GNSS, nous proposons d'utiliser un filtre de Kalman qui intègre un détecteur de rupture. L'estimateur proposé est appliqué à la réflectométrie GNSSR qui est une technique radar qui observe la surface de la terre à partir des signaux GNSS réfléchis. Dans ce travail nous estimons la réflectivité du signal GPS et nous détectons ces variations associées à des zones en eaux. On montre à partir du signal segmenté que 96% des zones en eaux sont détectés par le système radar aéroporté par un autogire. On montre aussi que la localisation des zones en eau est obtenu avec une précision métrique.

Abstract – This paper presents a model for the estimation of the GNSS signal amplitude using the signal correlation as an observation. We estimate the amplitude at the code repetition rate of the GPS C/A signal (1 ms rate). However, the model that links the in-phase component observations to the signal amplitudes at the 1 ms rate is non-linear. To estimate the amplitudes of the GNSS signals, we propose to use a Kalman Filter that incorporates a change detector. The proposed estimator is applied to GNSS-R which is a radar technique that provides observations of Earth surface from reflected GNSS signals. In this work, we estimate the GPS signal reflectivity and we detect the variations associated to the presence of water bodies. We show using signal segmentation, that 96% of the in-land water body surfaces are detected by the airborne radar system embedded on a gyrocopter while achieving the meter precision for water body edge localization.

1 Introduction

Global Navigation Satellite Systems - Reflectometry (GNSS-R) is a method of remote sensing which uses GNSS navigation signals as "Signals of Opportunity" in a bi-static radar system for Earth Observation. Its main principle is to receive and further extract information from the GNSS signals which are reflected off Earth surface in addition to those received directly from the satellites in order to derive some geophysical properties of Earth [1]. In GNSS-R, soil moisture content can be derived from the reflectivity measurements. These measurements are directly linked to the amplitudes of the GNSS signals.

In this regard, the Signal-to-Noise Ratio (SNR) can be used to observe the GNSS signal amplitudes. The SNR can be derived from the statistical properties of the in-phase and quadrature components of correlation. However, the maximum rate of SNR measurements that can be achieved in multi-bit quantization digital receivers is 20 ms in order to synchronize with the navigation message data bits [2].

In this paper, we propose a model that estimates the GNSS signal amplitudes (and therefore the SNR) at high rate, namely the code repetition rate (e.g. 1 ms for GPS C/A signals). We estimate the statistics of 1 sample over 1 ms in order to obtain 1 ms rate estimates of the GNSS signal amplitudes. The non-linear expression that links the maximum value of the in-phase component to the signal amplitude is derived. In order to estimate the time varying signals amplitudes, we propose a Kalman Filter to reverse the non-linear expression with the noisy observations of correlation provided by the tracking loops. A change detection system is utilized in order to detect the changes in the GNSS measurements obtained along a flight experimentation. The proposed model is applied in an airborne GNSS-R experiment for water body detection using a lightweight low altitude carrier.

2 GPS C/A front end processing

A GNSS software receiver processes the in-phase (I) and quadrature (Q) components of correlation with local replicas. In practice, GNSS receivers are numerical and the signals are frequency down converted with Analog-to-Digital Conversion (ADC) and quantization, and the local replicas are digitized. In our approach, 1-bit quantization is applied. We show in Figure 1, the processing block diagram of the in-phase component in a GNSS receiver front end.

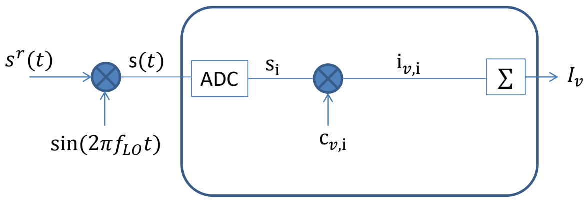

FIGURE 1 – Radio frequency GNSS receiver block diagram

The expressions of the signals in Figure 1 are defined after digitization by :

$$s_i = \left\lfloor \sum_{l \in V} A_l CA_l(t_i + \tau_l) \sin(2\pi f_l \, t_i + \phi_l) + \eta_i \right\rfloor_{>0} \quad (1)$$

$$c_{v,i} = \lfloor CA_v(t_i + \tau_v) \sin(2\pi f_v \, t_i + \phi_v) \rfloor_{>0} \quad (2)$$

where $c_{v,i}$ and s_i are respectively the local replica and the digitized sum of the signals. $\lfloor \ldots \rfloor_{>0}$ is a sign function that associates -1 to the negative values of the signal and +1 to positive (or zero) values. In the expression of s_i, V is the set of visible satellites. $A_l(t)$ is the amplitude of the signal, $CA_l(t)$ is the Code Division Multiple Access (CDMA) code of satellite l and τ_l is the code delay. f_l and ϕ_l are respectively the frequency and the phase delay of the carrier. $\eta(t)$ is a zero mean additive Gaussian noise with a unit variance. The in-phase component of the maximum of correlation I_v is obtained by accumulating the sampled signals over a coherent integration time T_c. Then we have :

$$I_v = \sum_{i=1}^{f_s \, T_c} s_i \, ci_{v,i} \quad (3)$$

Our aim is to derive an expression that links the amplitude A_v of the received signal to the mean value of the in-phase component. We define $i_{v,i} = s_i \, c_{v,i}$ to take the value +1 when s_i is equal to $c_{v,i}$ and -1 when they are different. Assuming that the random variables $i_{v,i}$ are identically distributed, we model the mean value of I_v as follows :

$$\begin{aligned} E(I_v) &= E(i_{v,i}) \, T_c f_s \\ &= (2 \, P(i_{v,i} = 1) - 1) \, T_c f_s \end{aligned} \quad (4)$$

where $T_c f_s$ is the number of samples integrated over a coherent integration time T_c.

3 Linearization of the measurement equation

Let us construct the following model approximation of the sampled signal of satellite v after digitization :

$$\hat{s}_i = \sum_{v \in V} A_v CA_v(t_i + \hat{\tau}_v) \sin(2\pi \hat{f}_v \, t_i + \hat{\phi}_v) \quad (5)$$

$$s_i \approx \lfloor \hat{s}_i + \eta_i \rfloor_{>0} \quad (6)$$

and

$$c_{v,i} \approx \left\lfloor CA_v(t_i + \hat{\tau}_v) \sin(2\pi \hat{f}_v \, t_i + \hat{\phi}_v) \right\rfloor_{>0} \quad (7)$$

where $c_{v,i}$ is defined to get the maximum of correlation. The probability of the random variable $i_{v,k}$ to take the value +1 is written as :

$$\begin{aligned} P\left(i_{v,i} = 1\right) &= P\left(c_{v,i} = 1\right) P\left(\eta_i \geq -\hat{s}_i / c_{v,i} = 1\right) \\ &+ P\left(c_{v,i} = -1\right) P\left(\eta_i < -\hat{s}_i / c_{v,i} = -1\right) \end{aligned} \quad (8)$$

An empirical estimate of the probability that the local replica is positive can be written as :

$$P\left(c_{v,i} = 1\right) = \frac{\sum_{i=1}^{f_s T_c} \left(c_{v,i} + 1\right)}{2 f_s T_c} \quad (9)$$

from which $P(c_{v,i} = -1)$ can be derived. An empirical estimate of the first probability of expression (8) associated to the additive random noise on the signal is defined as :

$$P\left(\eta \geq -\hat{s}_i / c_{v,i} = 1\right) = \frac{2}{\sum_{i=1}^{f_s T_c} \left(c_{v,i} + 1\right)} \sum_{\{\tilde{i}\}_v^1} P(\eta \geq -\hat{s}_i) \quad (10)$$

where the set $\{\tilde{i}\}_v^1$ defines the values of the index i as $i / c_{v,i} = 1$. The probability $P(\eta \geq -\hat{s}_i)$ is processed with the tabulated error function as follows :

$$\begin{aligned} \sum_{\{\tilde{i}\}_v^1} P(\eta \geq -\hat{s}_i) &= \sum_{\{\tilde{i}\}_v^1} \int_{-\hat{s}_i}^{+\infty} \frac{1}{\sqrt{2\pi}} exp(\frac{-x^2}{2}) \, dx \\ &= \sum_{\{\tilde{i}\}_v^1} \frac{1}{2} erfc\left(\frac{-\hat{s}_i}{\sqrt{2}}\right) \end{aligned} \quad (11)$$

The second probability estimate of expression (8) associated to the additive random noise on the signal can be derived as expression (10) over the set $\{\tilde{i}\}_v^2$ which defines the values of the index i as $i / c_{v,i} = -1$.

According to equations (4) and (8) we derive the following expression for the non-linear measurement function $f(\ldots)$:

$$f_{v,k}\left(\{A_{v,k}\}_{v\in V};\{\theta_{v,k}\}_{v\in V}\right)=\sum_{\{\tilde{i}\}^1_{v,k}} erfc\left(\frac{-\hat{s}_i}{\sqrt{2}}\right)$$
$$-\sum_{\{\tilde{i}\}^2_{v,k}} erfc\left(\frac{-\hat{s}_i}{\sqrt{2}}\right)+\sum_{i=1}^{f_sT_c}|c_{v,i}-1|-T_cf_s$$

where $\theta_{v,k}=\{\hat{\tau}_{v,k},\hat{f}_{v,k},\hat{\phi}_{v,k}\}$ denotes the GNSS signal parameters provided by the Phase Lock Loop (PLL) and Delay Lock Loop (DLL) components of the receiver. The GPS signal is very weak, so the values of $\hat{s}_i$ are small. Therefore, the following Taylor approximation of the tabulate function can be used in order to linearize the expression :

$$erfc(x)\approx 1-\frac{2}{\sqrt{\pi}}x \tag{12}$$

After simplification, we develop the expression of $\hat{s}_i$ to find a linear expression between $I_{v,k}$ and $A_{v,k}$. Accordingly, for a set V of n satellites in view, we have the following linear equation :

$$I_{V,k}\approx HA_{V,k}+\omega_k \tag{13}$$

with $I_{V,k}=[I_{1,k},\ldots,I_{n,k}]^T$ and $A_{V,k}=[A_{1,k},\ldots,A_{n,k}]^T$. H is a matrix that represents the contribution of the satellites in $I_{v,k}$ and ω_k is a Gaussian noise. We present in Figure 2 the different elements of H. For a component $I_{i,k}$, $h_{i,i}$ is the correlation contribution of the signal from satellite i and $h_{i,j}$ is the inter correlation contribution of the signal from satellite j. $h_{i,\forall j}$ is the global contribution of all the satellites in $I_{i,k}$. From the analysis of matrix H, the cross-correlation components $h_{i,j}$ contribute to the standard deviation of the random-like evolution of $E(I_v)$ approximately two times more than the contribution of the auto-correlation components $h_{i,i}$ [3].

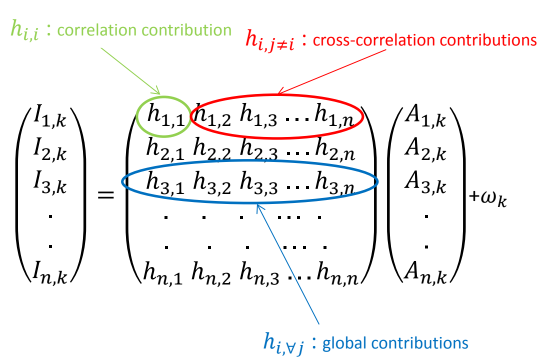

FIGURE 2 – Contribution of each satellite in the observations $I_{v,k}$.

4 Kalman estimate of the signal amplitude

We propose a state filter in the form of a Kalman Filter that uses the GNSS signal components as observations to provide $1\ ms$ rate estimates of the GNSS signal amplitudes. We assume that the amplitudes are constant during one period of the CDMA code. The state model is a classical second order state equation used for data smoothing where the second state is the rate of change of the first state.

In our airborne GNSS-R bi-static system, high rate reflectivity measurements are obtained as the ratio of the modulus of the amplitudes of the reflected signals A^r over the modulus of the amplitudes of the direct signals A^d as :

$$\Gamma(t)=\frac{A^r(t)}{A^d(t)} \tag{14}$$

A Kalman CUSUM approach is used to detect changes in the reflectivity measurements using the innovation of the filter. Then, a maximum likelihood localization approach is implemented for accurate geo-positioning of the edges of the scanned reflecting surfaces [4]. The proposed models are applied to airborne GNSS-R observation of in-land water body surfaces.

5 Experimentation

5.1 Water body detection

The proposed radar technique is first applied for in-land water body detection. Figure 3 shows the detected water body surfaces by our proposed radar technique over a study area between Guînes and Ardres imposed on IGN maps.

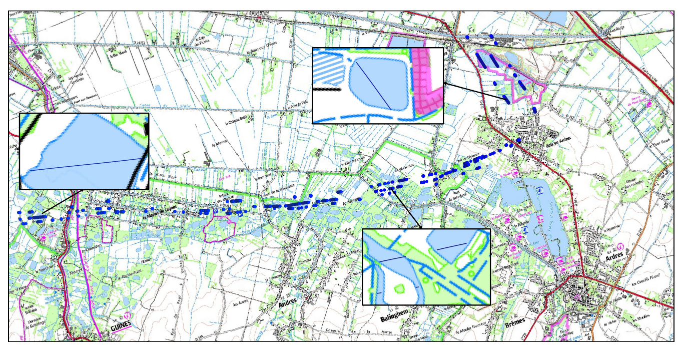

FIGURE 3 – The detected water body surfaces using our proposed radar technique for three satellites in study.

The radar technique detects 96% of in-land water bodies observed on IGN maps. However, the percentage of true water bodies detections, i.e. the number of times the proposed radar technique detects water when water is present on the map is 75%. Consequently, the percentage of false alarm detections, , i.e. the number of times the proposed radar technique incorrectly detects the presence of water is 25%. It is important to note that the percentage of false alarms is not strictly indicative of the radar technique detection accuracy because the results lack comparison with the ground truth especially that the flight took place in winter.

We show in Figure 4, the automatic segmentation of GNSS measurements by the proposed radar technique. The satellite traces are represented with specular point localization on Google Earth (Figure 4a). The segmentation model divides the signals into stationary segments based on the reflectivity measurements obtained for the different satellite signals (Figures 4b,4c,4d). As reflections are obtained from water bodies, the reflectivity increases allowing the detection of in-land water body surfaces associated with a blue coloring of the segments and of the corresponding specular points of reflection.

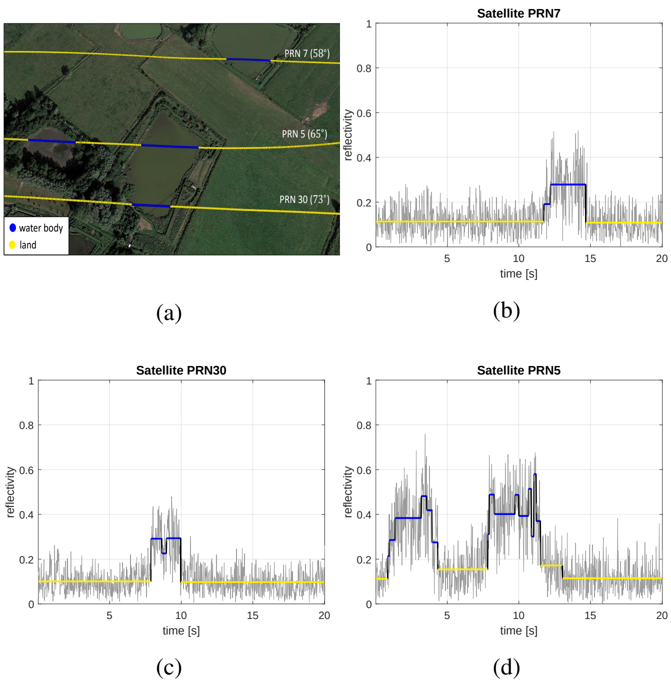

FIGURE 4 – Detection of in-land water body surfaces using the proposed automatic radar signal segmentation technique.

5.2 Water body edge localization

The radar signal segmentation system is also applied for water body edge localization. For that, we compare the manual edge localization via Google Earth with the automatic edge localization by the proposed radar technique. A total of 65 water body surfaces were detected along the traces of the three satellites in study. We show in Figure 5, the total number of perfect (absolute value of the offset between the 2 localization approaches is zero) and imperfect localizations along with the total number of edge localizations for the different water body surfaces.

From the histogram of Figure 5, the proposed radar technique achieves a total perfect edge localization percentage of 76.2%, i.e. 99 out of 130 possible perfect localizations. Furthermore, from the analysis of the water body edge localization accuracy, we observe a total mean distance localization error of $0.96\ m$ and a total localization difference standard deviation of

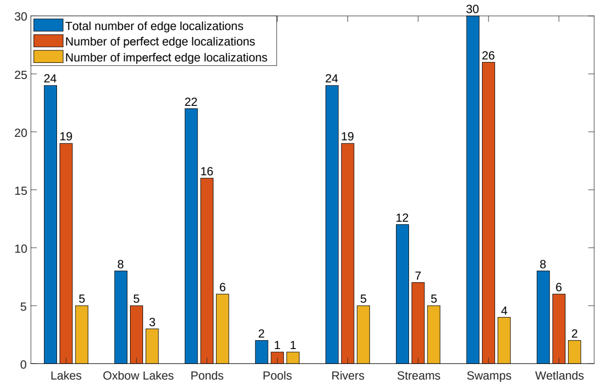

FIGURE 5 – Statistics of water body edge localization by the proposed radar technique per water body type.

$0.9\ m$. Therefore, we conclude that we can achieve the meter accuracy with our automatic localization approach as compared to manual localization using Google Earth.

6 Conclusion

In this article, we propose a high rate ($1\ ms$) estimator of the amplitudes of GNSS signals in the form of a Kalman Filter that uses $1\ ms$ rate of the in-phase components of the signals as observations. In order to be independent of the ambient temperature that affects the automatic gain control, 1-bit quantization digital receiver is used. The non-linear expression that links the maximum value of the in-phase correlation component to the signal amplitude is derived. The proposed model and filter inversion method are assessed on real airborne GNSS-R measurements. We apply a segmentation model to detect in-land water body surfaces along the flight trajectory. The proposed radar technique shows high detection capacity while localizing the edges of the detected surfaces with a meter accuracy.

Références

[1] Manuel Martin-Neira et al., "A passive reflectometry and interferometry system (paris) : Application to ocean altimetry," *ESA journal*, vol. 17, no. 4, pp. 331–355, 1993.

[2] Marco Pini et al., "Performance evaluation of C/N0 estimators using a real time GNSS software receiver," in *2008 IEEE 10th International Symposium on Spread Spectrum Techniques and Applications*. IEEE, 2008, pp. 32–36.

[3] Hamza Issa, Georges Stienne, Serge Reboul, Maximilian Semmling, Mohamad Raad, Ghaleb Faour, and Jens Wickert, "A probabilistic model for on-line estimation of the GNSS carrier-to-noise ratio"," *Signal Processing*, vol. 183, pp. 107992, 2021.

[4] Hamza Issa, Georges Stienne, Serge Reboul, Mohamad Raad, and Ghaleb Faour, "Airborne gnss reflectometry for water body detection," *Remote Sensing*, vol. 14, no. 1, pp. 163, 2021.